# Groundwater response to the tide in wetlands: Observations from the Gillman Marshes, South Australia

John A.T. Bye [a,*], Kumar A. Narayan [b,1]

[a] School of Earth Sciences, The University of Melbourne, Victoria 3010, Australia
[b] CSIRO Land and Water, GPO Box 1666, Canberra ACT 2601, Australia

## ARTICLE INFO

## ABSTRACT

We present results from a series of piezometers installed in the foreshore flat and mangrove environments of the Gillman Marshes, South Australia in an interdisciplinary study of the propagation of the ocean tide into the coastal aquifers. A unique feature of the analysis is that all water level records were harmonically analysed so that the behaviour of the four major tidal constituents could be independently examined. The main findings were that: (1) the decay of the groundwater tide in the coastal aquifers was greater than that predicted by the Ferris solution. A theoretical model has been developed and applied to the study site. The model suggests that this behaviour is due to the occurrence of a time delay in the Darcian response in the shelly and muddy sand substrate; (2) when the tide is incident over a gently sloping bank, the time delay in response gives rise to a spiked signal in which high water is confined to a small fraction of the tidal cycle; and (3) at the coastal interface tidal propagation across a sloping bank causes a rise in the water table relative to mean sea level which is proportional to the variance of tidal elevation and inversely proportional to the decay constant of the groundwater tide. The model developed in this study is also applicable to other coastal groundwater systems with tidal influence.

© 2009 Elsevier Ltd. All rights reserved.

## 1. Introduction

An aquifer, hydraulically connected to an open water body undergoing periodic changes in head, transmits the fluctuations inland, causing groundwater levels and hydraulic gradients to fluctuate continuously. Several studies, e.g. Carr and van der Kamp (1969), Erskine (1991) and Smith and Hick (2001), have investigated the tidal signal. The key finding was that the propagation of the tidal fluctuations through the aquifer did not agree with the simple diffusive theory, originally proposed by Ferris (1951), in which the propagation of sinusoidal fluctuations in head in a confined homogeneous aquifer along $0x$ is governed by the equation,

$$\partial h / \mathrm{d}t = \beta \partial^2 h / \partial x^2 \qquad (1)$$

where $t$ is time, $h$ is the groundwater head, and $\beta = T/S$ is the diffusivity of the aquifer in which $S$ is the storage coefficient and $T$ is the transmissivity (Bear and Verruijt, 1987). In (1) the time derivative of head is balanced uniformly by diffusion due to the hydraulic conductivity and storativity of the medium (Li and Jiao, 2003).

Here we present and interpret a series of observations, obtained in both a mangrove and a foreshore environment of a tidal inlet, which gives a new insight into the physics of tidal propagation in coastal aquifer systems. Wolanski (2007) provides an excellent summary of the nature of these environments, however the link between the constituents of the open sea tide and those of the groundwater tide, including that between the mean water level in the sea and in the aquifer does not appear to have been previously established.

The observational site is the Gillman Marshes in the Port River estuary, South Australia (Fig. 1), which was the focus of a groundwater study undertaken by the Centre for Groundwater Studies and CSIRO Land and Water between October 1991 and March 1993 (Pavelic and Dillon, 1993), of which the tidal observations formed an important component. The unique feature of the tidal

* Corresponding author.
  *E-mail addresses:* jbye@unimelb.edu.au (J.A.T. Bye), kumar.narayan@csiro.au (K.A. Narayan).
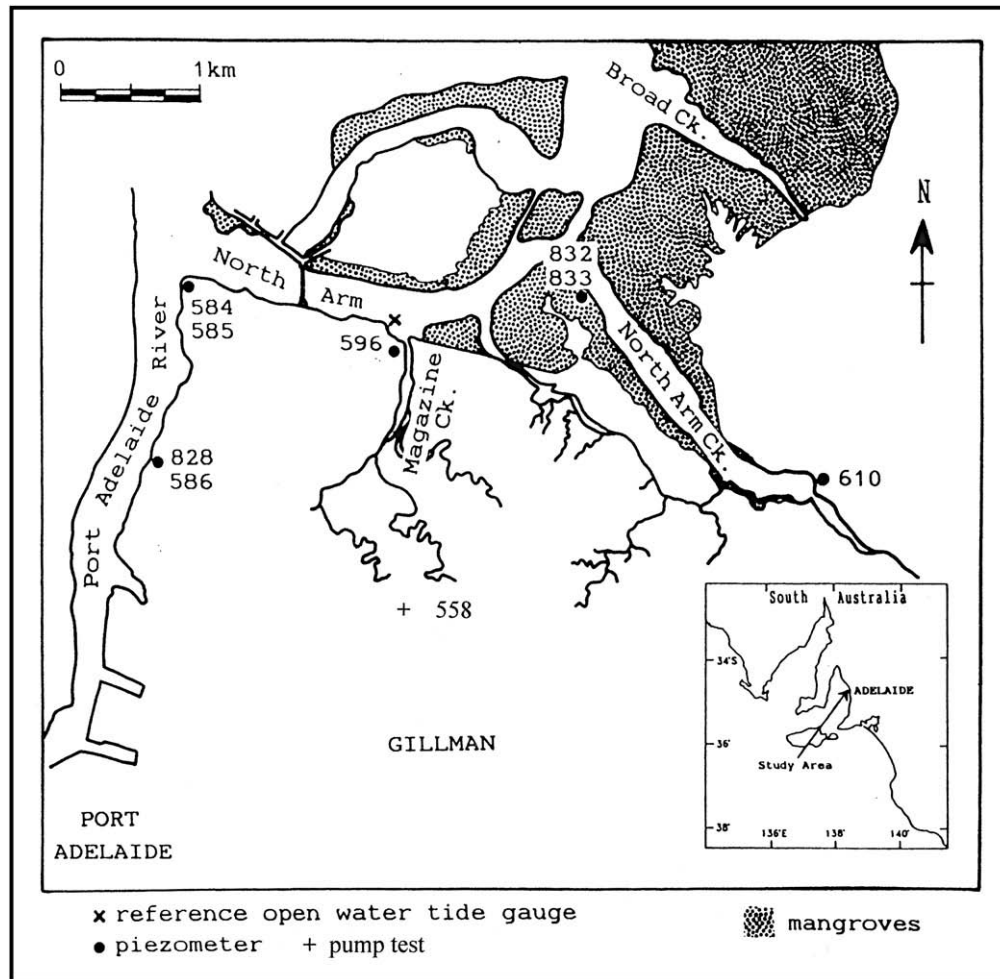  [1] Tel.: +61 2 6246 5874; fax: +61 2 6246 5965.

**Fig. 1.** Map of the Gillman Marshes, South Australia (adapted from Pavelic and Dillon (1993)).

observations, obtained from a series of piezometers installed adjacent to the shoreline, was that the tidal signal was harmonically analysed into tidal constituents, the phase and amplitude of which could be compared with their values in the open water. This paper presents the first hydrodynamical interpretation of the results.

It is worth emphasizing that there are very few investigations of the tidal influences on groundwater systems in coastal aquifers (Li and Jiao, 2003), and that in all previous studies the tidal signal has been considered as being essentially a single constituent and hence the variation in response with frequency could not be determined.

Section 2 describes the oceanography (Section 2.1) and hydrogeology (Section 2.2) of the study site, and also points out how the work can be regarded as a component of the larger groundwater study (Section 2.3) of this important region within 5 km of Port Adelaide, which is a major centre of infrastructure for South Adelaide. The core of the study (which is supported by Appendix 1) consists of the solution for tidal propagation into the coastal aquifer over a sloping bank (Section 3.2), which includes the prediction of the mean water level in the aquifer relative to mean sea level. In Section 3.3 a hydrological model is introduced from which the diffusivity of the aquifer can be computed using the results of the harmonic tidal analysis. The analysis is applied briefly to two historical data sets in Section 4, and in Section 5 some general aspects of the study are discussed.

## 2. The Gillman Marshes

### 2.1. Oceanography

The tides of the South Australian Sea have been extensively studied (Middleton and Bye, 2007). The principal feature in the open water adjacent to the study site is that the dominant semi-diurnal constituents ($M_2$ and $S_2$) have approximately equal amplitudes of about 0.5 m (Table 1). This results in an exaggerated spring-neap cycle. The two most important diurnal constituents ($O_1$ and $K_1$) also make a significant contribution to the observed tide (which is classified as mixed), and in addition there are significant meteorological storm surges which propagate with the synoptic systems along the south coast of Australia. A series of detailed oceanographic studies of the tides of the Port River estuary have also been made, which are summarized in Bye and Kämpf (2008). Fig. 2 shows a segment of the tidal record obtained from the reference open water station at the mouth of Magazine Creek (Fig. 1) used in this study, which clearly shows the semi-diurnal spring-neap cycle which arises from the beating of the $M_2$ and $S_2$ constituents and has a period of 14.8 days. The tidal constituents (Table 1) have been obtained from a high quality harmonic analysis of the tidal record made in the National Tidal Facility of the Bureau of Meteorology, Australia (originally housed in Flinders University).

**Table 1**
Tidal constants for the Magazine Creek reference open water tide gauge and the piezometers (adapted from Smith (1993)). M: Magazine Creek reference open water tide gauge, cs coarse sand, ms muddy sand, ss shelly sand, x: distance from shoreline at mean sea level, d: depth of piezometer, L length of record. The pairs of piezometers 828 & 586, 584 & 585, and 832 & 833 are situated at the same sites, and calcrete layers occur between the first two pairs at 7.3 m and 7.6 m respectively. a (m) and g ($^0$) are respectively the amplitude and phase of the tidal constituent.

| | $O_1$ | | $K_1$ | | $M_2$ | | $S_2$ | | L | x | d | |
|---|---|---|---|---|---|---|---|---|---|---|---|---|
| | a | g | a | g | a | g | a | g | days | m | m | |
| | m | 0 | m | 0 | m | 0 | m | 0 | | | | |
| M | 0.17 | 30 | 0.24 | 53 | 0.50 | 119 | 0.50 | 190 | 289 | | | |
| 828 | 0.008 | 160 | 0.008 | 178 | 0.005 | 255 | 0.004 | 332 | 170 | 40 | 0.91 | cs |
| 586 | 0.110 | 40 | 0.156 | 67 | 0.314 | 133 | 0.316 | 207 | 170 | 40 | 11.18 | cs |
| 584 | 0.083 | 69 | 0.087 | 105 | 0.141 | 162 | 0.131 | 232 | 89 | 40 | 0.83 | cs |
| 585 | 0.067 | 54 | 0.103 | 78 | 0.168 | 146 | 0.175 | 221 | 89 | 40 | 9.51 | ms |
| 596 | 0.031 | 74 | 0.044 | 103 | 0.058 | 177 | 0.060 | 250 | 93 | 50 | 4.45 | ms |
| 832 | 0.005 | 49 | 0.006 | 108 | 0.006 | 137 | 0.008 | 211 | 68 | 100 | 0.28 | ss |
| 833 | 0.009 | 117 | 0.014 | 143 | 0.008 | 183 | 0.010 | 210 | 55 | 90 | 1.00 | ss |
| 610 | 0.020 | 90 | 0.021 | 137 | 0.024 | 194 | 0.020 | 256 | 83 | 80 | 6.81 | ss |

## 2.2. Hydrogeology

The Gillman Marshes are situated within about 5 km of Port Adelaide, South Australia, and are bounded by the Port River (which is Adelaide's main shipping channel) to the west, and by North Arm Creek to the east (Fig. 1). The area consists of low lying marshland, with original mangrove swamps still existing in the intertidal zones of North Arm Creek. Much of the western half has been reclaimed, while levee banks around the northern perimeter prevent overland tidal inundation in the remaining areas.

Belperio (1985) and Belperio and Rice (1989) who conducted detailed analyses of thirty-five cores from the Gillman site and surrounds, found that the surficial aquifer consists of marine and fluvial Quaternary sediments between 5 m and 11 m thick, deepening towards the north-west; and for water balance calculations Pavelic and Dillon (1993) assume that the thickness of the Gillman marine aquifer is 9 m. It is underlain by a 70 m thick layer of essentially impermeable Hindmarsh clay and silts. Within the aquifer are two layers, both marine sequences of different age. The lower layer is the Glanville formation, comprising mainly sandy sediments interspersed with fossils and shells, which lies on the Hindmarsh clay and rises to −1 m AHD (Australian Height Datum) in the north-east grading to −10 m AHD near the Port River. The upper layer is the St Kilda formation, whose composition varies significantly (Belperio and Rice, 1989) with a strip 500 m wide, adjoining the Port River which consists of shelly and muddy sands, the remaining area comprising muddy or sandy peat. Hydraulic conductivities, determined from slug and laboratory core tests, range from ∼0.5 m/day in the sands to ∼0.02 m/day in the muddy peat (Pavelic and Dillon, 1993). A pump test in a sandy soil profile at Site 558 (Fig. 1) yielded a diffusivity of 3300 m$^2$ day$^{-1}$.

## 2.3. Hydrological investigations

Fifty-four piezometers were installed in the Gillman–Dry Creek area by the Centre for Groundwater Studies as part of an investigation of groundwater levels and water quality (Pavelic and Dillon, 1993). The groundwater levels were recorded at 30 min intervals and the record lengths of the eight piezometers used in this study (Fig. 1) varied between 55 and 170 days (Table 1). The piezometers consisted of 40 mm PVC pipes, driven vertically into the aquifer at depths up to 13 m. A band of narrow vertical slots in each pipe 30 mm long and beginning 100 mm from its base provided the hydraulic connection with the aquifer, and the sides of the pipe were carefully repacked to prevent vertical leakage.

The mean water table as determined from these observations in March 1993 (Fig. 3) shows an evaporative basin west of North Arm Creek protected by levee banks to the north, and elevations of about 0.2 m AHD around the coastline except for North Arm Creek where they are about 0.6 m. This pattern was found to be representative of conditions occurring at other times of the year (Pavelic and Dillon, 1993).

The records from the piezometers, which were harmonically analysed in an identical manner to the reference open water tidal record, fall into two groups. The first group, located in the foreshore flat environment, consisted of five piezometers, 586, 584, 585, and 596, which showed level fluctuations resembling the open water tide (Fig. 4), and piezometer 828, which displayed an almost non-tidal response. The second group (832, 833 and 610), located in a mangrove environment, showed water level fluctuations, which were characterized by sharp, non-sinusoidal peaks (Figs. 5 and 6), which are characterized by a spring-neap cycle due to the beating of the $K_1$ and $O_1$ constituents with a period of 13.6 days. In this paper, we present a unified theory for both groups.
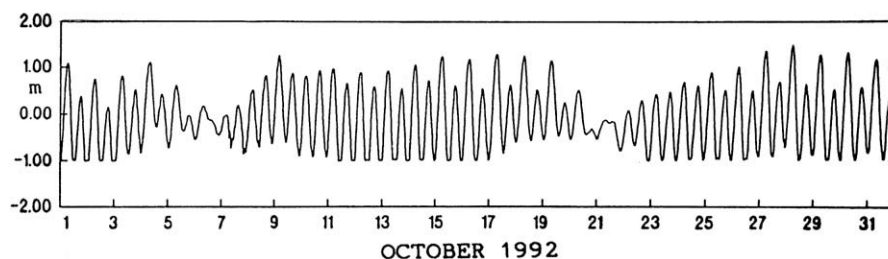


**Fig. 2.** Tidal record from the mouth of Magazine Creek for October 1992.
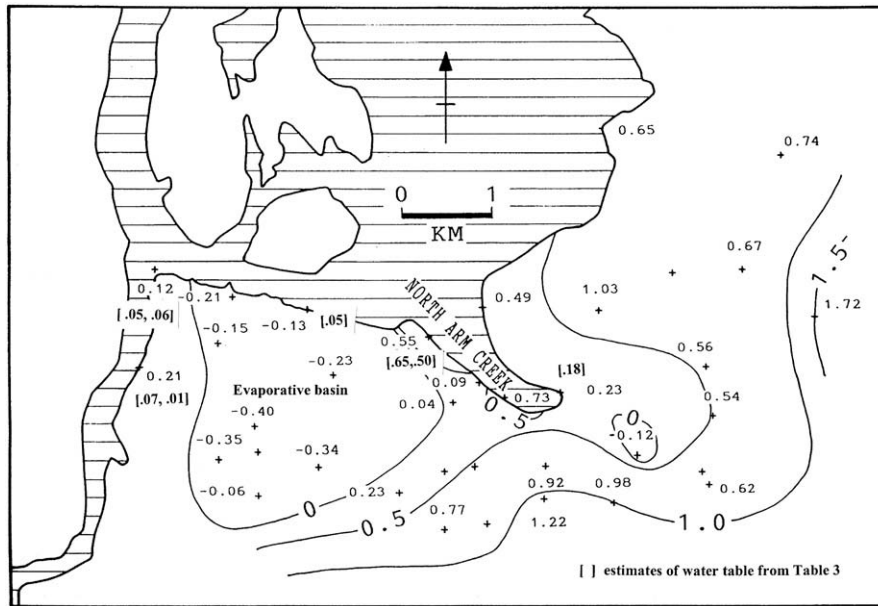
**Fig. 3.** Contours of piezometer head in the Gillman Marshes on March 26 1993 (from Pavelic and Dillon (1993)).

## 3. Analysis

### 3.1. Specification of the groundwater tide

We interpret the piezometer observations by assuming that each open water tidal constituent,

$$h_t = a_0 \cos(\sigma t - g_0) \tag{2}$$

of angular frequency, $\sigma$, and amplitude, $a_0$, and phase, $g_0$, propagates into the aquifer along an inward normal to the coast $(0x)$ as a damped oscillation of amplitude,

$$a = a_0 \cos(\sigma t - kx - g)e^{-\theta x} \tag{3}$$

where $g$ is the phase, which is identical with the open water tidal constituent at $x = 0$, at which $g = g_0$ and has a wavenumber $(k)$ and a decay constant $(\theta)$. At $x$, we have the amplitude ratio (tidal efficiency),

$$R = a/a_0 = \exp(-\theta x) \tag{4a}$$

and also the phase lag,

$$\Delta g = g - g_0 = kx \tag{4b}$$

which yield $k = \Delta g/x$ and $\theta = -\ln R/x$. Table 1 shows $a$ and $g$, and Table 2 shows the determinations of $k$ and $\theta$, for the eight piezometers from the harmonic analysis for the four major tidal constituents, $M_2$, $S_2$, $K_1$ and $O_1$, respectively of angular frequency, $\sigma$, 28.98, 30.00, 15.04 and 13.94°/mean solar hour, or of period, $T$ ($=2\pi/\sigma$), 12.42, 12.00, 23.93 and 25.82 h.

The most important result (see Table 1) is that the ratios of the mean amplitude of the diurnal and the semi-diurnal constituents for group 1 (excluding piezometer 828) and for group 2 are respectively 0.50 and 0.99, which highlights the diurnal character of the group 2 records. This is due to the corresponding ratios of the mean decay constants, 0.80 and 0.76 (see Table 2), although similar, being <1, and hence the greater mean distance (90 m) of the group 2 compared with that (42.5 m) of the group 1 piezometers greatly attenuates the semi-diurnal relative to the diurnal constituents. The parameter $(A = \theta/k)$ is a non-dimensional decay parameter for the wave. The results (with few exceptions) show that $A \sim 2$ for all piezometers, except piezometer 832 for which $A \sim 10$, the reason for which is not fully understood.

### 3.2. Theory for tidal ingress over a sloping bank

The shape of the aquifer wave is determined, in addition to the propagation of the damped oscillations (3), by any harmonic tides which are generated within the aquifer. The primary mechanism is the ingress of the tide over the sloping beach through which the open water high water occurs further inland than the low water. This imparts a non-linearity to the response of the aquifer in which the damped oscillation is modified in an analogous process to that
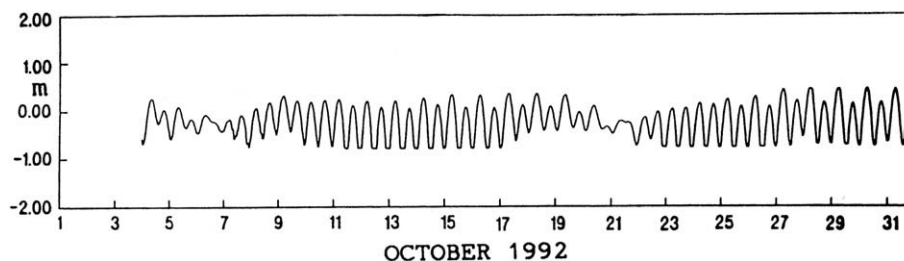


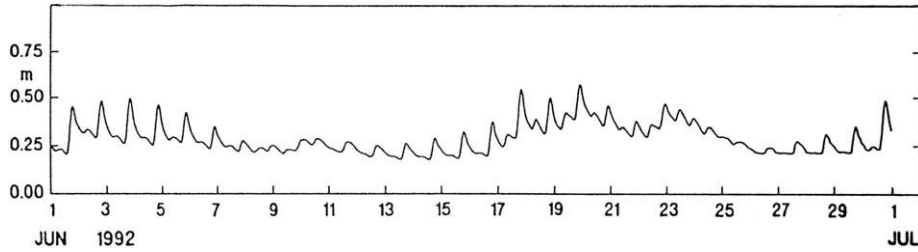**Fig. 4.** Groundwater record from Piezometer 586 for October 1992.

**Fig. 5.** Groundwater record from Piezometer 832 for June 1992.

occurring in finite-amplitude ocean waves, although of course the resultant waveform (which after its generation by the sloping beach propagates inland within the aquifer) is different.

A mathematical statement is that the boundary condition which links the ocean and groundwater tides must be applied at different positions depending on the stage of the tide, i.e.

$$h_t = h(x, t) \tag{5}$$

where for a linear bank,

$$x = h_t \cot s \tag{6}$$

in which $s$ is the bank slope, and for the tidal constituent (2), $x = 0$, at the mid-tide coordinate. A method of applying the boundary condition (5) to determine the groundwater tide has been developed by Nielsen (1990) in an investigation of the tidal dynamics of a sloping beach. We apply this method here assuming that the groundwater signal consists of a summation of decaying progressive waves of the form (3),

$$h(x, t) = b_0 + \sum_{j=1,\infty} b_j \cos\left(j\sigma t - kx - \psi_j\right) e^{-\theta x} \tag{7}$$

in which the amplitudes $(b_j)$ and the phases $(\psi_j)$ are to be determined. On matching the tidal elevation at $x$, and assuming for convenience that $g_0 = 0$, we obtain,

$$a_0 \cos \sigma t = b_0 + \sum_{j=1,\infty} b_j \cos\left(j\sigma t - \varepsilon\cos \sigma t - \psi_j\right) e^{-A\varepsilon\cos \sigma t} \tag{8}$$

where $A = \theta/k$ and,

$$\varepsilon = ka_0 \cot s \sim ka_0/s \tag{9}$$

where $\varepsilon$ is a small parameter (see Table 3), which is a measure of the finite-amplitude response. On equating coefficients in (8) and considering terms to order $\varepsilon^2$ $(O(\varepsilon^2))$, we obtain the solution (A1) of Appendix 1. The leading terms of $O(1)$ and $O(\varepsilon)$ are the following:

$$b_0 = 1/2a_0 A\varepsilon = 1/2a_0^2 \theta/s \tag{10a}$$

$$b_1 = a_0, \quad \psi_1 = 0 \tag{10b}$$

$$b_2 = 1/2a_0\left(A^2 + 1\right)^{1/2}\varepsilon, \quad \psi_2 = \tan^{-1}(-1/A) \tag{10c}$$

$$b_j = 0, \quad j > 2 \tag{10d}$$

where the $O(1)$ term is the damped oscillation (3). This solution indicates that, as the bank slope decreases a first harmonic overtide $(b_2)$, which has the same decay constant as its parent tide, and also a positive mean water level relative to the mean sea level $(b_0)$ are generated. An important property of the solution is that for small bank slopes the groundwater tide is distorted towards a spiked signal in which high water is confined to a small fraction of the tidal cycle. As the non-dimensional decay parameter increases the phase of the overtide tends to that of the primary tide, and hence the spiked signal becomes more symmetric, as is shown in the respective records (Figs. 5 and 6) for piezometer 610 (A ∼ 2) and piezometer 832 (A ∼ 10).

This behaviour can be monitored by comparing the $M_2$ tide with the shallow water tide, $M_4$, which has exactly double the frequency of $M_2$, and is also included in the harmonic tidal analysis (Table 3). $M_4$ will be due partly to the propagation into the aquifer of the shallow water tide from the open water, and partly to generation within the aquifer. Hence, in order to apply the prediction (10c) it is necessary to estimate the component due to the propagation of the shallow water tide into the aquifer. Fortunately the amplitudes of the open water $M_4$ constituent (Table 3) suggest that it is of minor importance. This was checked by estimating $\varepsilon$ using,

$$a_G(M_4)/a(M_2) \approx 1/2\left(A^2 + 1\right)^{1/2}\varepsilon \tag{11}$$

where $a_G(M_4)$ is the amplitude of the aquifer generated $M_4$ tide, assuming: (1) the $M_4$ shallow water tide propagates into the aquifer with the same values of $k$ and $\theta$ as for $M_2$; and (2) the shallow water tide is of negligible importance in the aquifer. The results (Table 3)
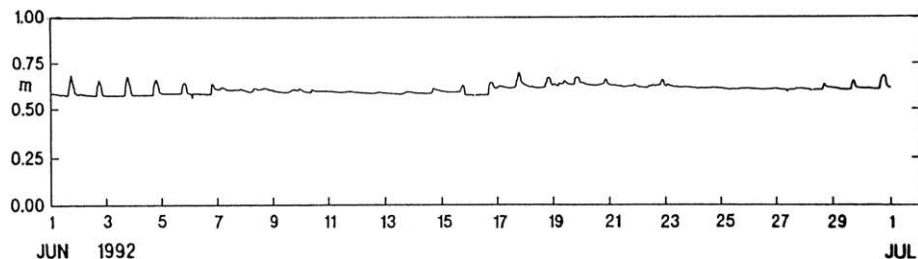


**Fig. 6.** Groundwater record from Piezometer 610 for June 1992.

**Table 2**
Parameters of the groundwater tide.

| | $O_1$ | | | $K_1$ | | | $M_2$ | | | $S_2$ | | |
|---|---|---|---|---|---|---|---|---|---|---|---|---|
| | $k$ | $\theta$ | $A$ | $k$ | $\theta$ | $A$ | $k$ | $\theta$ | $A$ | $k$ | $\theta$ | $A$ |
| | $m^{-1}$ | $m^{-1}$ | | $m^{-1}$ | $m^{-1}$ | | $m^{-1}$ | $m^{-1}$ | | $m^{-1}$ | $m^{-1}$ | |
| 828 | 0.057 | 0.078 | 1.4 | 0.055 | 0.085 | 1.6 | 0.059 | 0.115 | 1.9 | 0.062 | 0.120 | 2.0 |
| 586 | 0.005 | 0.011 | 2.5 | 0.006 | 0.011 | 1.7 | 0.006 | 0.012 | 1.9 | 0.008 | 0.011 | 1.4 |
| 584 | 0.017 | 0.018 | 1.1 | 0.023 | 0.025 | 1.1 | 0.018 | 0.032 | 1.7 | 0.019 | 0.033 | 1.8 |
| 585 | 0.011 | 0.024 | 2.3 | 0.011 | 0.021 | 1.9 | 0.012 | 0.027 | 2.3 | 0.014 | 0.026 | 1.9 |
| 596 | 0.015 | 0.035 | 2.3 | 0.018 | 0.035 | 1.9 | 0.020 | 0.043 | 2.1 | 0.021 | 0.042 | 2.0 |
| 832 | 0.003 | 0.036 | 10.9 | 0.010 | 0.037 | 3.9 | 0.003 | 0.045 | 14.5 | 0.002 | 0.041 | 21.5 |
| 833 | 0.017 | 0.032 | 1.9 | 0.017 | 0.031 | 1.8 | 0.012 | 0.046 | 3.7 | 0.004 | 0.043 | 11.2 |
| 610 | 0.013 | 0.027 | 2.0 | 0.018 | 0.030 | 1.6 | 0.016 | 0.038 | 2.3 | 0.015 | 0.040 | 2.8 |

show that for all piezometers, $\varepsilon$, is a small parameter justifying the neglect of higher order terms in (10a–d), and also that the estimates of $\varepsilon$ are generally insensitive to the propagation parameters.

On using the results from model (1), and substituting $a$ and $k$ from the $M_2$ tide into (9), the effective bank slope ($s$) (Table 3) shows that large bank slopes are associated with the main group of piezometers in the foreshore flat environment, and the small bank slopes are associated with the other group in the mangrove environment. Unfortunately no direct measurements of bank slope are available, however reference to Fig. 2 suggests that the estimates of $s$ are not unrealistic, and at spring tides in which the tidal amplitude, $a_s \approx \Sigma_{i=1,4} (a_0)_i$, where $(a_0)_i$ is the amplitude of the open water tidal constituent, the linear bank slope model can be used to estimate the maximum tidal inundation relative to the mean sea level, $I_{max} = a_s/s$. For $a_s = 1.42$ m (Table 1), in the foreshore flat environment the mean $I_{max} = 6$ m, and in the mangrove environment the mean $I_{max} = 40$ m, both values being significantly less than the respective distances ($x$) of the piezometers from the shoreline (Table 1).

Using the estimates of $s$ the mean water level ($W$) at the piezometer sites can be calculated from (10a) by summing over each of the four tidal constituents ($i = 1,4$), which yields $W = \frac{1}{2}\Sigma_{i=1,4} ((a_0)_i^2 \theta_i)/s$. Fig. 3 indicates that there is good agreement between the observed water table and $W$ (Table 3) in the mangrove environments, where $s$ is small, but in the foreshore flat environment, where the mean water table is only slightly elevated above mean sea level, $W$, is too small, possibly due to the overestimation of $s$ by the linear bank slope model. The effect of the finite amplitude of the tide within the aquifer has also been neglected. This gives rise to an additional rise in mean water table, $b_P = [(1 + \frac{1}{2}(a_0/H)^2)^{1/2} - 1]H$, where $a_0$ is the tidal amplitude and $H$ is the aquifer thickness (Philip, 1973). On summing over the four tidal constituents with $H = 9$ m, see Section 2.2, we obtain $b_P = 0.016$ m, which is

small compared with the mean water level ($W$) in the mangrove environment, but of similar magnitude in the foreshore flat environment.

These results strongly support the applicability of the sloping bank model with respect to the generation of the $M_4$ tide and also the elevation of mean level. This suggests that the spiked diurnal tidal signal of the group 2 piezometers arises from the same mechanism, even though the frequencies of the semi-diurnal constituents are not exactly double the frequencies of the diurnal constituents. The key physics is that at the distance of the piezometers from the shoreline, the propagation of the semi-diurnal constituents from the open water is of negligible importance compared to their generation within the aquifer as follows from their greater decay constants. Hence the amplitude and phase of the semi-diurnal tide are determined by (10c) applied to the diurnal tide as the fundamental oscillation, see Appendix 2.

It is interesting that the spiked tidal signal of piezometer 832 (Fig. 5) is reminiscent of that occurring in tidal propagation in the St Lawrence River at Grondines and Cap à la Roche where the momentum balance, which is between the pressure gradient and bottom friction, yields a parabolic equation for the tidal velocity ($u$) of the form (1) in which the diffusivity is $(1/2 \, gH^2/(KU))$ and $H$ and $U > u$ are respectively the river depth and velocity and $K$ is the bottom drag coefficient (LeBlond, 1978). Although the generation mechanism may be completely different, it is intriguing that in both instances an overtide is generated which leads the fundamental tide by about 25° and is of about 35% its amplitude.

### 3.3. The hydrological model

The results of the piezometer analysis can be interpreted using a simple hydrological model in which a delay in the diffusive adjustment of head by Darcy flow is introduced into the Dupuit equation. The solution of (1) for a constant ($\beta$), obtained by Ferris (1951) for the wave, $h = h_0 \cos \sigma t$, incident at $x = 0$, is,

$$h = h_0\cos(\sigma t - kx)e^{-kx} \tag{12a}$$

which has the properties that the wavenumber and decay parameter are equal ($A = 1$), and

$$k = (1/2\sigma/\beta)^{1/2} \tag{12b}$$

This model is inadequate to describe our results, see Table 2.

A simple modification of (1) in which

$$(\partial h/\partial t)_t = \beta \left(\partial^2 h/\partial x^2\right)_{t-\tau} \tag{13}$$

which indicates that the diffusive response is delayed by $\tau > 0$, can be used to simulate the observed results. On solving (13) for $A$ as a function of $\tau$, see Appendix 3, we obtain,

**Table 3**
Aquifer and environmental properties at the piezometer sites. M: Magazine Creek reference open water tide gauge. (i) and (ii) estimates of $\varepsilon$ respectively using model (1) and model (2), see Section 3.2.

| | $M_4$ | | $\varepsilon$ | | s | W | $\beta_T$ |
|---|---|---|---|---|---|---|---|
| | a | g | (i) | (ii) | | m | m² day⁻¹ |
| | m | 0 | | | | | |
| M | 0.0051 | 204 | | | | | |
| 828 | 0.0003 | 342 | 0.047 | 0.061 | 0.63 | 0.05 | 650 |
| 586 | 0.0042 | 42 | 0.022 | 0.012 | 0.14 | 0.02 | 67000 |
| 584 | 0.0070 | 263 | 0.041 | 0.048 | 0.22 | 0.04 | 7800 |
| 585 | 0.0059 | 127 | 0.031 | 0.042 | 0.19 | 0.04 | 13800 |
| 596 | 0.0019 | 332 | 0.027 | 0.028 | 0.37 | 0.04 | 5500 |
| 832 | 0.0022 | 258 | 0.048 | 0.054 | 0.032 | 0.59 | 6400 |
| 833 | 0.0037 | 309 | 0.235 | 0.241 | 0.026 | 0.48 | 5800 |
| 610 | 0.0041 | 309 | 0.126 | 0.136 | 0.063 | 0.18 | 6900 |

$$A = \tan G + \left(1 + \tan^2 G\right)^{1/2} \tag{14}$$

where $G = \sigma\tau$ is the phase lag of the diffusive response, and also,

$$k = \left[1/\left(A^2 + 1\right)\sigma/\beta\right]^{1/2} \tag{15}$$

Thus an increase in the non-dimensional decay parameter is due to a corresponding increase in the delay of the diffusive response. The phase lag ($G$) is $0°$ for $A = 1$ (The Ferris solution) and increases to $37°$ for $A = 2$ and $79°$ for $A = 10$.

Equation (15) enables the components of diffusivity for each tidal constituent ($\sigma$) to be estimated from $A$ and $k$ (Table 2). Clearly, however, a single value of diffusivity ($\beta_T$) characterizes the aquifer, which can be estimated from the complete tidal signal using the rms estimate, derived by summing over the four tidal constituents ($i = 1,4$),

$$\beta_T = \left[\sum_{i=1,4}(a_i\sigma_i)^2 / \sum_{i=1,4}\left(a_i\left(A_i^2 + 1\right)k_i^2\right)^2\right]^{1/2} \tag{16}$$

in which the contribution of each groundwater tidal constituent ($a_i$) is weighted by its amplitude, and on the assumption that $\beta_T$ is independent of $\sigma$, i.e. the diffusivity is a property of the aquifer, we obtain the predictive relation,

$$k = \left[1/\left(A^2 + 1\right)\sigma/\beta_T\right]^{1/2} \tag{17}$$

which is analogous to (12b) of the Ferris solution. Table 3 shows that $\beta_T \sim 6000$–$14,000 \text{ m}^2 \text{ day}^{-1}$, irrespective of bank slope with a mean value of $7700 \text{ m}^2 \text{ day}^{-1}$, except for the pair of piezometers 828 and 586 which are situated at the same site (Fig. 1) where $\beta_T$ is small for the shallow and large for the deep piezometer. On substituting $\beta_T = 7700 \text{ m}^2 \text{ day}^{-1}$, in (17), we obtain for the semi-diurnal tidal constituents, $k = 0.018 \text{ m}^{-1}$ ($A = 2$) and $k = 0.004 \text{ m}^{-1}$ ($A = 10$), and for the diurnal tidal constituents, $k = 0.013 \text{ m}^{-1}$ ($A = 2$) and $k = 0.003 \text{ m}^{-1}$ ($A = 10$), which are in good general agreement with the observations (Table 2), suggesting that the delayed diffusion model is a reasonable representation of the aquifer physics.

The somewhat smaller diffusivity from the pump test, see Section 2.2, compared with the mean diffusivity from the tidal measurements may reflect the smaller measurement scale on which the pump test was conducted, relative to that of the tidal signal.

## 4. Other data sets

Two historical data sets are also suitable for a single constituent tidal analysis. Firstly, at Sizewell in East Anglia in the United Kingdom (Erskine, 1991) where the geology consists of a highly permeable sand sequence overlying bedrock, the oscillations in head from a series of 12 piezometers between 25 m and 300 m from the coast yielded estimates of $\theta$ and $k$ for the dominant $M_2$ constituent, which predict a significant delay in the diffusive response ($A = 3.3$) and a large diffusivity ($\beta = 1.8 \times 10^5 \text{ m}^2 \text{ day}^{-1}$). Secondly, in the confined coastal aquifers on Prince Edward Island, Canada, data were collected (Carr and van der Kamp, 1969) around Charlottetown in a region where the groundwater moves through fractures between sandstone and siltstone facies. Here, the tidal analysis indicated that for 4 out of 11 aquifers, the non-dimensional decay parameter ($A$) is less than unity, which is arguably consistent with a fractional medium response, and that $\beta$ varies widely over the range, $2 \times 10^4$–$10^6 \text{ m}^2 \text{ day}^{-1}$. This suggests that the modified Dupuit equation (13) can be used for flow in a wide variety of aquifers, although clearly many more comprehensive data sets are required to test this hypothesis.

## 5. Conclusions

This study has been primarily concerned with the propagation of the ocean tide into a coastal aquifer. The main thrust of the analysis has been to show that the observations can be interpreted using a general hydrodynamical theory rather than by recourse to inhomogeneities in the aquifer, except as they cause a delay (or an advance) in the diffusive response, see Section 3.

The tidal analysis indicates that the groundwater tide can be represented as a sum of tidal constants in a similar manner to the open sea tide, a key feature being the development of tidal harmonics which lead to a groundwater tide in which high water is confined to a spike over a small fraction of the tidal cycle. This response, which is favoured by a small bank slope, and a muddy or shelly sand aquifer in which water retention precludes an instantaneous adjustment to changes in head, arises from the boundary condition with the open sea over the sloping bank rather than any non-linear processes. This boundary condition is also responsible for the setup in the water table in the coastal aquifer relative to mean sea level, which may act as a control on groundwater discharge from the intertidal, (especially mangrove) swamps into the open sea. In particular (10a) suggests a basic dynamical model for the intertidal zone, in which an increase in the height of the water table, (possibly due to flood conditions) with no change in the decay constant for the tidal propagation into the aquifer, could in the long run give rise to a new equilibrium of smaller bank slope, and over a shorter period impede the propagation of the tide into the aquifer by increasing the decay constant ($\theta$). These simple ideas may possibly be incorporated in a morphological model of intertidal swamps, in which one-dimensional propagation over a linear bottom slope is relaxed and replaced by more general conditions. The implications for the marine ecology of the high water spikes and the setup are also beyond the scope of this paper, and remain to be investigated.

## Appendix 1. Solution for groundwater head on a linearly sloping bank to $0(\varepsilon^2)$

The solution of (8) to $0(\varepsilon^2)$ is,

$$
\begin{aligned}
h(x,t) = &\; 1/2 a_0 A\varepsilon + a_0 \cos(\sigma t - kx)e^{-\theta x} \\
&+ 1/2 a_0 \varepsilon \left(A^2 + 1\right)^{1/2}\cos\left(2\sigma t - kx - \tan^{-1}(-1/A)\right)e^{-\theta x} \\
&+ 1/4 a_0 \varepsilon^2 \left(A^2 + 1\right)\left[\sin\left(3\sigma t - kx - \tan^{-1}(-1/A)\right.\right. \\
&\left.- \tan^{-1} A\right) + \sin\left(\sigma t - kx - \tan^{-1}(-1/A) - \tan^{-1} A\right)\bigg] \\
&e^{-\theta x} - 1/8 a_0 \varepsilon^2 \bigg[\left(A^2 + 1\right)\sin\left(3\sigma t - kx - \tan^{-1}\right. \\
&\left(1/2\left(A^2 - 1\right)/A\right)\bigg) + \left(9A^4 - 14A^2 + 9\right)^{1/2} \\
&\sin\left(\sigma t - kx - \tan^{-1}\left(3/2\left(A^2 - 1\right)/A\right)\right)\bigg]e^{-\theta x}
\end{aligned}
\tag{A1}
$$

which includes the fundamental and the first and second harmonic terms.

Equation (A1) was derived following the method of Nielsen (1990) which consisted of equating terms in a Taylor expansion of $O(\varepsilon^2)$, and in the limit of $A \to \infty$, which is approximately valid for the observations (especially for piezometer 832) simplifies to the expression,

$$h(x,t) \approx 1/2a_0A\varepsilon + a_0\cos(\sigma t - kx)e^{-\theta x}$$
$$+ 1/2a_0A\varepsilon\cos(2\sigma t - kx)e^{-\theta x} + 1/4a_0A^2\varepsilon^2\cos(\sigma t - kx)e^{-\theta x} \tag{A2}$$

in which the second harmonic term is insignificant.

## Appendix 2. The generation of the diurnal spiked tidal response

The amplitude of the diurnal tide in the aquifer,

$$a_D = \sum_{i=1,2} a_i\cos \sigma_i t \tag{B1}$$

where $a_i$ and $\sigma_i$ are respectively the amplitude and frequency of the two diurnal constituents, and it has been assumed for convenience that their phases are both zero. Around spring tide, which is centred on $t = 0$, $K_1$ and $O_1$ reinforce each other, and $\cos \sigma_i t \approx 1 - 1/2\sigma_i^2t^2$, and hence,

$$a_D \approx \langle a\rangle\cos\langle \sigma\rangle t \tag{B2}$$

where $<a> = a_1 + a_2$ and $<\sigma>^2 = (a_1\sigma_1^2 + a_2\sigma_2^2)/<a>$. Hence, as the amplitudes of $K_1$ and $O_1$ are similar for each of the group 2 piezometers (Table 1), $<\sigma>$ is approximately diurnal, and (10c) generates a semi-diurnal constituent, which is phase locked to the fundamental, and for a small bank slope leads to a spiked diurnal response.

## Appendix 3. The delayed diffusive response solution

From (3), we assume that,

$$h = h_0\cos(kx - \sigma t')e^{-Akx} \tag{C1}$$

where $t' = t - \tau$, and hence,

$$\partial^2 h/\partial x^2\big)_{t'} = h_0k^2\left[\left(A^2 - 1\right)\cos(kx - \sigma t') + 2A\sin(kx - \sigma t')\right]e^{-Akx} \tag{C2}$$

and,

$$\partial h/\partial t\big)_{t'+\tau} = \sigma h_0[\cos G\sin(kx - \sigma t') + \sin G\cos(kx - \sigma t')]e^{-Akx} \tag{C3}$$

where $G = \sigma\tau$, and on substituting (C2) and (C3) in (13) and equating coefficients of $\cos(kx - \sigma t')$ and $sin(kx - \sigma t')$, we obtain (15) and also $A^2 - 2A \tan G - 1 = 0$ and hence (14).

## References

Bear, J., Verruijt, A., 1987. Modelling Groundwater Flow and Pollution. Reidel, Dordrecht, 414 pp.

Belperio, A.P., 1985. Site Investigations in the Vicinity of the Dean Rifle Ranges, Port Adelaide Estuary. Geological Survey. Dept. Mines and Energy, South Australia.

Belperio, A.P., Rice, R.L., 1989. Stratigraphic Investigation of the Gillman Development Site, Port Adelaide Estuary. Dept. Mines and Energy, South Australia.

Bye, J.A.T., Kämpf, J., 2008. Physical oceanography. In: Shepherd, S.A., Bryars, S., Kirkegaard, I., Jennings, J.T. (Eds.), Natural History of Gulf St Vincent. Royal Society of South Australia, pp. 56–70.

Carr, P.A., van der Kamp, G.S., 1969. Determining aquifer characteristics by the tidal method. Water Resources Research 5, 1023–1031.

Erskine, A.D., 1991. The effect of tidal fluctuations on a coastal aquifer in the UK. Groundwater 29, 556–562.

Ferris, J.G., 1951. Cyclic fluctuations of a water level as a basis for determining aquifer transmissivity. International Association of Scientific Hydrology Publication 33, 148–155.

LeBlond, P.H., 1978. On tidal propagation in shallow rivers. Journal of Geophysics Research 83 (C9), 4717–4721.

Li, H., Jiao, J.J., Review of analytical studies of tidal groundwater flow in coastal aquifer systems. Proc. of Intl. Symp. on Water Resources & the Urban Environment, November 9–10, 2003, Wuhan, PR China. pp. 86–91.

Middleton, J.F., Bye, J.A.T., 2007. A review of the shelf-slope circulation along Australia's southern shelves; Cape Leeuwin to Portland. Progress in Oceanography 75, 1–14.

Nielsen, P., 1990. Tidal dynamics of the water table in beaches. Water Resources Research 26, 2127–2134.

Pavelic, P., Dillon, P.J., 1993. Gillman–Dry Creek Groundwater Study. Centre for Groundwater Studies. Report No. 54 (two volumes).

Philip, J.R., 1973. Periodic nonlinear diffusion: an integral relation and its physical consequences. Australian Journal of Physics 26, 513–519.

Smith, A., 1993. Tidal analysis and modeling of fluctuations in an unconfined aquifer. B.Sc. (Hons) Thesis Flinders University, South Australia. 61 pp.

Smith, A.J., Hick, W.P., 2001. Hydrogeology and Aquifer Tidal Propagation in Cockburn Sound, Western Australia. CSIRO Technical Report 6/01.

Wolanski, E., 2007. Estuarine Ecohydrology. Elsevier, Amsterdam, 157 pp.